

NEUTRON CAPTURE AND TOTAL CROSS SECTION MEASUREMENTS OF CADMIUM AT THE RPI LINAC

G. Leinweber*, D. P. Barry, R. C. Block, J. A. Burke, M. J. Rapp, and K. E. Remley

Bechtel Marine Propulsion Corporation

P.O. Box 1072, Schenectady, NY, 12301-1072 USA

leinwg@rpi.edu, barryd3@rpi.edu, blockr@rpi.edu, jburkesr@nycap.rr.com, rappm@rpi.edu, and
RemleyKE@unnpp.gov

Y. Danon

Department of Mechanical, Aerospace & Nuclear Engineering

Rensselaer Polytechnic Institute

110 8th St. Troy, NY 12180-3590 USA

danony@rpi.edu

ABSTRACT

Cadmium has been used historically as an important component of integral experiments because of its high thermal neutron absorption cross section. Correct interpretation of such experiments depends on accurate Cd differential neutron cross section measurements. The 60-MeV electron accelerator at the Gaertner LINAC Center was used to generate neutrons for neutron capture and total cross section measurements of natural Cd. Measurements were performed in the thermal and epithermal resonance range with sample thicknesses ranging from 1×10^{-4} to 4×10^{-2} atoms per barn. A full resonance region analysis was performed in order to determine the thermal cross sections and resonance integrals of the cadmium isotopes. The Bayesian R-Matrix code SAMMY 8.0 was used to shape fit the data and extract the resonance parameters. Resonance parameter and cross section uncertainties were determined from their primary components: transmission background, capture normalization, experimental resolution function, burst width, sample thickness, and counting statistics. The experiments were analyzed for consistency within the measured capture and transmission using multiple sample thicknesses. Results are compared to previously published measurements and evaluated nuclear libraries. No major changes to the thermal cross section or the first resonance in Cd113 were identified from the consensus achieved from measurements and evaluations over the past decade.

KEYWORDS

Cadmium, Transmission, Capture, Thermal

1. INTRODUCTION

Cadmium is a strong absorber of thermal energy neutrons; the 2200 m/s cross section of Cd113, 12.2% abundant in natural Cd, is $\sim 20,000$ barns. As such it has been used to cover activation foils to quantify the epithermal flux in nuclear criticality benchmarking experiments. It is a material used in neutron activation experiments and wherever the removal of virtually all thermal neutrons is desired. In addition the shape of the cross section on the high energy side of the first resonance is very important to accurate calculation of the Cd cut. Therefore, precise measurements of its thermal cross section shape, and thus the underlying resonance parameters have been undertaken.

The suite of natural cadmium transmission and capture measurements were performed in 2002 and 2003, then repeated in 2007. The consistency of the results have thus been verified not only with samples of multiple thicknesses in independent but overlapping energy regions (thermal and epithermal), but also over a span of years using different time-of-flight (TOF) clocks, analysis codes, and analysts. At the time the current measurements commenced there was some uncertainty in the resonance parameters of the prominent resonance at 0.178 eV in Cd113. However, as a result of the current measurements and those of Kopecky[1], a consensus has emerged.

A more extensive discussion of this measurement including comparisons with previous measurements and evaluated nuclear data libraries is available in Reference 2.

2. EXPERIMENTAL CONDITIONS

2.1. Experimental Details

The details of the experiments are given in Table I including neutron targets, overlap filters, LINAC pulse repetition rates, and flight path lengths. The nominal resolution, pulse width divided by flight path length, was ~ 2 ns/m for the epithermal experiments. Thermal measurements did not require fine energy resolution. A crucial parameter in each data analysis is the resonance energy at which the transmission background or the capture flux is normalized. This resonance for each measurement is given in Table I.

The electron linear accelerator at Rensselaer Polytechnics Institute's (RPI) Gaertner LINAC Center was used to bombard Ta plates in a neutron-producing target. The neutron-producing targets were optimized for each energy range.[3,4,5] Sample placement was automated. All samples were cycled into the neutron beam approximately every hour. In addition to the main data-taking detector, a separate set of neutron detectors operated on an adjacent beamline to measure fluctuations in the neutron beam intensity from sample-to-sample. These data are referred to as beam monitor data and are used to make a small adjustment to the data from the main data-taking detectors.

The zero time for the measured time-of-flight spectrum was determined from a separate measurement of the location of the count rate peak produced by the flash of gamma rays which accompanies each pulse of electrons from the accelerator. This 'gamma flash' coincides with each burst of neutrons from the target.

2.2. Sample Information

Each experiment subjected a series of sample materials to a neutron flux for the purpose of determining the interaction rate in the sample. Details of the Cd samples and the experiments in which they were used are given in Table II. Sample thicknesses ranged from approximately 1.1×10^{-4} to 4.4×10^{-2} atoms per barn. Thick samples were needed to see a significant number of reactions in weak resonances. Thin samples were needed to get optimum transmission for strong resonances. The samples were 50.8 mm in diameter. The uncertainties in sample thicknesses were determined from mass and multiple diameter measurements. The diameter measurements were the primary source of uncertainty in sample thickness. The samples had a nominal purity of 99.99%. A spectrographic analysis of the samples yielded the impurities above 1 ppm as 4 ppm Pb and 3 ppm Au.[6]

Table I. Cadmium Experimental Details

Experiment	Overlap Filter	Neutron-Producing Target	Electron Pulse Width (ns)	Ave. Beam Current (μA)	Beam Energy (MeV)	Pulse Repetition Rate (pulses/s)	Flight Path Length (m)	Normalization Point for Transmission Background or Capture Flux (eV)
Epithermal Transmission	Boron Carbide	Bare Bounce	53 \pm 3	22	56	225	25.589 \pm 0.007	45 eV resonance in Mo95 fixed notch
Thermal Transmission Week 1 of 3	None	Enhanced Thermal Target	1900 \pm 100	12	50	25	14.973 \pm 0.004	18.8 eV resonance in W186
Thermal Transmission Week 2 of 3			920 \pm 50	6	55			5.2 eV resonance in Ag109
Thermal Transmission Week 3 of 3			900 \pm 70	6	60			
Epithermal Capture Week 1 of 2	Boron Carbide	Bare Bounce	49 \pm 2	23	52	225	25.564 \pm 0.006	27 eV resonance in Cd111 in the 200-mil sample
Epithermal Capture Week 2 of 2			48.3 \pm 0.1		54			
Thermal Capture Week 1 of 2	None	Enhanced Thermal Target	1400 \pm 100	11	50	25	25.444 \pm 0.004	0.178 eV resonance in Cd113 in 20-mil sample data
Thermal Capture Week 2 of 2			770 \pm 40	8.5	54			

Table II. Sample Details

Nominal thickness (mm)	Areal density (atoms/barn)	Measurements
0.0254 (0.001 in.)	$1.133 \times 10^{-4} \pm 1 \times 10^{-7}$	Thermal capture
0.0508 (0.002 in.)	$2.329 \times 10^{-4} \pm 2 \times 10^{-7}$	Thermal transmission and capture
0.1016 (0.004 in.)	$4.280 \times 10^{-4} \pm 4 \times 10^{-7}$	Thermal transmission and capture, and epithermal capture
0.254 (0.010 in.)	$1.180 \times 10^{-3} \pm 1 \times 10^{-6}$	Thermal transmission and epithermal capture
0.508 (0.020 in.)	$2.393 \times 10^{-3} \pm 2 \times 10^{-6}$	Thermal and epithermal transmission, Thermal and epithermal capture
1.27 (0.050 in.)	$5.853 \times 10^{-3} \pm 6 \times 10^{-6}$	Epithermal capture
2.54 (0.100 in.)	$1.191 \times 10^{-2} \pm 1 \times 10^{-5}$	Epithermal transmission
5.08 (0.200 in.)	$2.430 \times 10^{-2} \pm 3 \times 10^{-5}$	Epithermal transmission and capture
10.16 (0.400 in.)	$4.426 \times 10^{-2} \pm 5 \times 10^{-5}$	Epithermal transmission

2.3. Capture Detector

Capture measurements were made with the same detector for thermal and epithermal energy ranges using the time-of-flight (TOF) method at an approximately 25.5 m flight path. The capture detector is a gamma-ray detector consisting of 20 liters of NaI(Tl) divided into two annular right circular cylinders whose axes were parallel with the neutron beam. Each detector half was divided into 8 pie-shaped, optically-isolated segments.[7] The inside of the annulus is lined with a 1.0-cm thick annulus of 99.5 wt% B10 carbide ceramic to reduce the number of scattered neutrons reaching the gamma detector. A total energy deposition of 1 MeV for the epithermal measurement and 2 MeV for the thermal measurement was required to register a capture event. Therefore, the system discriminates against the 478 keV gamma rays from B10(n; α , γ) absorptions. The maximum dead time correction was 8.5%.

2.4. Transmission Detectors

Transmission measurements were made using two separate Li6 glass detectors. Thermal measurements were made at ~15 m using a 7.62-cm (3-in) diameter, 0.3-cm-thick NE 905 Li6 glass scintillation detector (6.6% lithium, enriched to 95% in Li6) coupled to a single photomultiplier. Data from the thermal experiment were analyzed from a few meV to ~10 eV. Cd samples (see Table II) and empty aluminum sample holders were cycled in and out of the neutron beam.

Epithermal measurements were made at ~25.6 m with a 12.70-cm (5-in.) diameter, 1.27-cm-thick Li6 glass scintillator (with similar Li content and enrichment as the thermal detector) housed in a light-tight aluminum box.[8] Two photomultiplier tubes were positioned out of the neutron beam to collect the scintillation light. Data from the epithermal experiment were analyzed from 15-1000 eV.

The transmission can be expressed as the ratio of the count rate with a sample in the beam to the count rate with samples removed once all count rates have been corrected for background. The transmission can vary strongly with incident neutron energy and is directly linked to the total cross section of the sample material being measured. The maximum dead time correction was 3%.

3. DATA REDUCTION

Raw data were corrected for dead time, normalized to the beam monitors, summed over all cycles, background subtracted, and processed into transmission or yield. Transmission is the fraction of the beam that is uncollided after interaction with the sample. Yield is defined as the number of neutron captures per neutron incident on the sample. The data processing methods, and analytical techniques are similar to those used for other measurements from the RPI LINAC for Eu[9], Dy[10], and Re[11].

The energy dependent neutron flux shape was measured separately using a 2.54-mm thick, 98.4% enriched $^{10}\text{B}_4\text{C}$ sample. The total energy deposition discriminator setting was set to a window from 360-600 keV in order to record the 478 keV gamma ray from neutron absorption in ^{10}B . To avoid dead-time concerns only two of the 16 NaI segments were active. For the epithermal capture measurement the flux shape measured in this way was corrected for the transmission through the boron carbide sample. The measured flux shape was normalized to a ‘black’ (saturated) resonance in Cd. The resonance used for this normalization was located at an energy of 0.178 eV for thermal capture or 27 eV for epithermal capture, as shown in the rightmost column of Table I. The detector efficiency for a typical gamma cascade was approximately 90%.¹⁰ No provision was made for the detector efficiency in the analysis since the flux was normalized to a black resonance in Cd113. Most of the fitted resonances were from the even-odd nuclei Cd111 and Cd113 with similar binding energies whose efficiencies are expected to be similar. The dead time of the system was set to 1.125 μs . The background in the capture measurements was determined from in-beam measurements of empty sample holders.

The background in the transmission measurements was measured explicitly at the black resonance of a ‘fixed’ notch, a filter placed in the beam throughout the Cd measurements for the express purpose of providing a normalization point for the background shape. The energy dependent background shape was determined by a separate series of experiments that consisted of a package of black resonance filters placed in the neutron beam. The notch thickness and black resonances for thermal measurements included 0.91-mm of cadmium at 0.178 eV, 0.25-mm of indium at 1.4 eV, 0.18-mm of silver at 5.2 eV, and 0.13-mm of tungsten at 18.8 eV. The notch thicknesses and black resonances for epithermal measurements included 0.18-mm silver at 5.2 eV, 0.13-mil tungsten at 18.8 eV, 0.25-mil cobalt at 130 eV, and 1.0-mm of an 80 weight % Mn, 20 weight % Cu alloy at 336 eV. Single- and double-thicknesses of these notch filters were placed in the beam and measured with each Cd sample as well as open beam. The one-notch and two-notch data were used to extrapolate to zero-notch thickness.[12] The resulting background shape was normalized to the fixed notch given in the rightmost column of Table I.

4. RESULTS

The SAMMY 8.0[13] Bayesian multi-level R-matrix code was used to extract resonance parameters from the neutron capture and transmission data. The analysis employed the experimental resolution, Doppler broadening, self-shielding, multiple scattering, and propagated uncertainty parameter features of SAMMY. The resulting resonance parameters of cadmium up to 100 eV are listed in Table III. The first four columns are resonance energies and uncertainties, the next four columns are radiation widths and uncertainties, then four columns of neutron width information, followed by isotope, spin and parity (J^π), and angular momentum (ℓ). The measured value, the Bayesian and external uncertainties, and the ENDF/B-VII.1 values[14] are given in Table III for each of the resonance parameters: resonance energy, neutron width, Γ_n , and radiation width, Γ_γ . The external uncertainties are the weighted standard deviation of individual sample fits and represent the sample-to-sample consistency within the current data.[2,9,10,11]

Table III. Resonance parameters for Cd compared with ENDF/B-VII.1 parameters. Two uncertainties are given for each parameter, the Bayesian uncertainty from the SAMMY fit and an external error, in brackets, which conveys the agreement among individual sample fits.

E, eV	ΔE	Eendf	Γ_γ	$\Delta \Gamma_\gamma$	Γ_γ endf	Γ_n	$\Delta \Gamma_n$	Γ_n endf	J^π	ℓ	
	Bayesian [external]			Bayesian [external]		Bayesian [external]		isotope			
-700		-11.7800	110		112	700		0.4485	108	0.5	0
-550		-195.8600	37		50.34	3000		177.0000	116	0.5	0
-225		-400.5400	55		50	100		2000.0000	114	0.5	0
-125		-12.1640	100		76	870		3.4390	112	0.5	0
-100		-97.4250	180		160	120		129.7000	106	0.5	0
-20		-9.5698	110		73	40		9.6580	110	0.5	0
-4		-27.9430	68		129	1		187.3000	111	1.0*	0
0.1779	0.00002 [0.0002]	0.1787	112.4	0.03 [0.4]	113.5	0.6379	0.0003 [0.008]	0.6336	113	1.0	0
4.56	0.09	4.5630	163		163	0.0014	0.0009	0.0014	111	-1.0	1
6.95	0.06	6.9546			143			0.0009	111	-2.0	1
7.0	0.1	7.000			160			0.0002	113	-1.0	1
18.362	0.002 [0.002]	18.365	95		95	0.181	0.002 [0.004]	0.1880	113	1.0	0
21.87	0.03 [0.02]	21.831	82		82	0.0054	0.0005 [0.0001]	0.0057	113	-2.0	1
27.5567	0.0005 [0.0007]	27.570	131		131.1	4.88	0.01 [0.07]	4.9120	111	1.0	0
28.97	0.01 [0.004]	28.979	70		70	0.030	0.001 [0.0001]	0.0269	116	-1.5	1
43.4	0.1 [0.009]	43.380	128		128	0.0039	0.0004 [0.0001]	0.0038	113	-2.0	1
49.76	0.07 [0.01]	49.770	160		160	0.064	0.005 [0.0005]	0.0600	113	0.0	1
54.24	0.05 [0.01]	54.200	115		115	0.18	0.01 [0.0008]	0.1575	108	-1.5	1
56.10	0.05 [0.02]	56.230	169		169	0.055	0.005 [0.0002]	0.0537	113	-1.0	1
56.353	0.009 [0.005]	56.425	72		71.5	0.033	0.001 [0.0008]	0.0375	114	-1.5	1
63.688	0.001 [0.002]	63.700	90		90	3.22	0.02 [0.04]	3.4667	113	1.0	0
66.759	0.0008 [0.001]	66.780	63		62.8	8.04	0.03 [0.07]	8.4760	112	0.5	0
69.56	0.01 [0.01]	69.590	130		130	0.170	0.007 [0.004]	0.1760	111	1.0	0
81.5	0.2 [0.004]	81.520	113		113	0.0045	0.0004 [0.0001]	0.0043	113	-2.0	1
82.42	0.02 [0.008]	82.466	90		90.5	0.039	0.002 [0.0006]	0.0409	112	-1.5	1
83.289	0.005 [0.004]	83.315	90		90.5	0.176	0.003 [0.003]	0.1870	112	-1.5	1
84.855	0.001 [0.002]	84.910	144	2 [2]	110	31.3	0.1 [0.5]	29.8670	113	1.0	0
86.165	0.002 [0.003]	86.185	130		130.1	3.10	0.02 [0.02]	3.3540	111	1.0	0
89.515	0.001 [0.002]	89.549	75	0.4 [1]	73.18	159	0.4 [1]	162.7000	110	0.5	0
98.3	0.1 [0.03]	98.520	225		225	0.044	0.003 [0.0001]	0.0336	113	-2.0	1
99.450	0.001 [0.002]	99.491	130		129.6	14.4	0.06 [0.2]	14.5700	111	1.0	0

* The ENDF/B-VII.1 J^π for this resonance is 0.0

A graphical overview of the thermal data, the SAMMY fit representing the current (NNL/RPI) resonance parameters, and those from ENDF/B-VII.1 in the thermal region are shown in Fig 1. The 2200 m/s cross section for Cd113 is 20051 ± 14 barns. The capture resonance integral for Cd113 is 383 ± 1 barn. These values are dictated by the fit to the strong resonance in Cd113 at 0.178 eV. The value could also be influenced by the presence of negative energy resonances, also known as bound levels. There are no negative energy resonances in Cd113 in either of the evaluated nuclear data libraries, ENDF/B-VII.1, JEFF-3.2[15], or JENDL-4.0[16]. The best fit to the 0.178 eV resonance data slightly underestimates the transmission for the 0.10 mm Cd sample at 0.0253 eV, see Fig. 1. It can be seen from Fig. 1 that the transmission of this sample at 0.0253 eV is approximately 0.3. This sample is one of the most sensitive since it is thick enough to show a deep resonance in transmission without as much reliance on the background fit as thicker samples with transmissions near zero.[17] No negative energy resonance was added for Cd113 because an additional resonance would move the calculated transmission lower and not improve the fit. The contributions from the other resonances to the thermal cross section of natural Cd is $\ll 1\%$. Therefore, none of the negative energy resonances were fitted. The JENDL-4.0 negative energy resonances were adopted because they gave the best fit to all of the data.

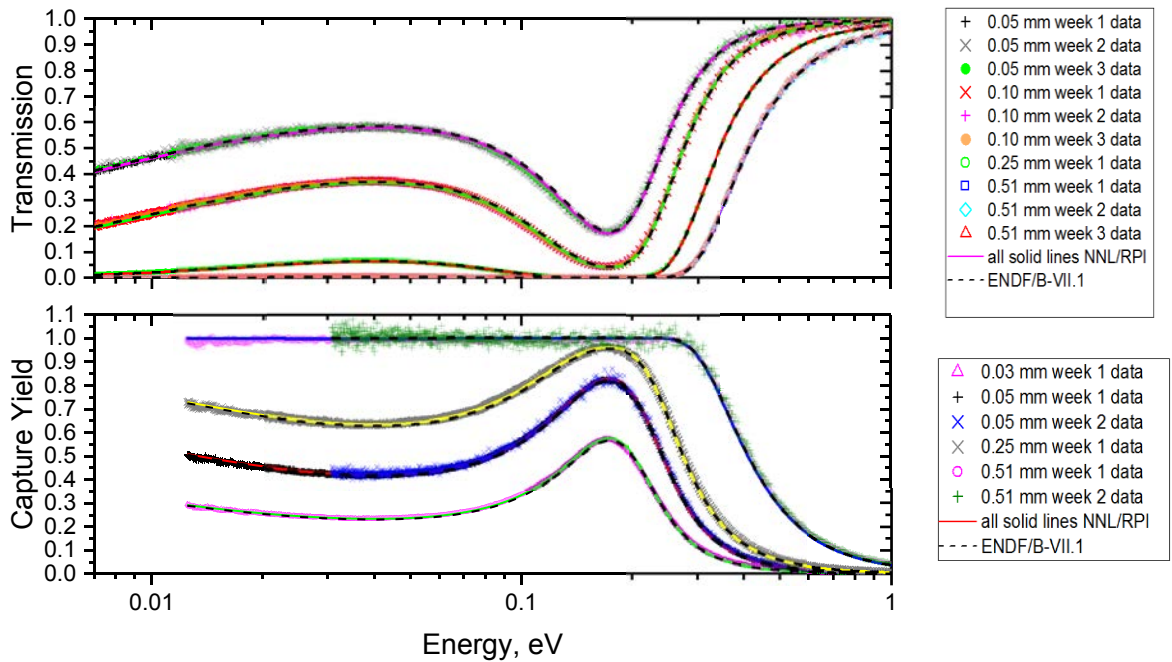


Figure 1. Overview of the thermal Cd transmission (top) and capture data (bottom) and curves calculated using NNL/RPI and ENDF/B-VII.1 resonance parameters. The samples are natural Cd. The thermal value is dictated by the 0.178 eV resonance in Cd113.

The resonance parameter fit with the SAMMY code included a description of the experimental resolution and an uncertainty propagation from 8 specific sources. The resolution function differed for capture, thermal transmission, and epithermal transmission measurements. The sources of experimental uncertainty were resolution function, normalization, background, flight path length, zero time, burst width, sample thickness, and effective temperature. The effective temperature used in the analysis was 298.9 K. More results including fits and resonance parameters up to 1 keV, staircase plots of level densities, strength functions, reduced neutron width distribution comparisons to Porter Thomas, average

radiation widths for particular isotopes and spins, capture resonance integrals, and thermal total cross sections are given in Reference 2.

5. CONCLUSIONS

The current measurements of neutron capture and transmission provide resonance parameters, thermal cross sections, and capture resonance integrals of cadmium. The neutron width of the 0.178 eV resonance in Cd113 agrees within uncertainties with the most recent experiment of Kopecky[1] as well as the current evaluated nuclear libraries ENDF/B-VII.1, JEFF-3.2, and JENDL-4.0.

The capture resonance integral of Cd113 from the current measurement agrees with the ENDF/B-VII.1 value and is closer to JENDL-4.0 and the Atlas[18] than it is to JEFF-3.2.

The thermal cross section of Cd113 overwhelms the contributions from all other isotopes of natural Cd. The current measurements give a thermal cross section for Cd113 that is within the measured uncertainty of the JENDL-4.0 value and within 1% of the ENDF/B-VII.1 and JEFF-3.2 values.

6. ACKNOWLEDGEMENTS

We thank the LINAC staff for both operating the accelerator during these measurements and providing us with the mechanical and electronic assistance we needed.

REFERENCES

1. S. KOPECKY, I. IVANOV, M. MOXON, P. SCHILLEBEECKX, P. SIEGLER, I. SIRAKOV, "The total cross section and resonance parameters for the 0.178 eV resonance of ^{113}Cd ," *Nucl. Instrum. Meth. B*, **267**, pp. 2345–2350 (2009).
2. G. LEINWEBER, D. P. BARRY, R. C. BLOCK, J. A. BURKE, K. E. REMLEY, M. J. RAPP, and Y. DANON, "Cadmium Resonance Parameters from Neutron Capture and Transmission Measurements of Cadmium at the RPI LINAC," arXiv:1801.03424v1 [nucl-ex] (2018).
3. Y. DANON, R. E. SLOVACEK, and R. C. BLOCK, "The Enhanced Thermal Neutron Target at the RPI LINAC," *T. Am. Nucl. Soc.*, **68**, 473 (1993).
4. Y. DANON, R. E. SLOVACEK, and R. C. BLOCK, "Design and Construction of a Thermal Neutron Target for the RPI LINAC," *Nucl. Instrum. Meth. A*, **352**, 596 (1995).
5. M. E. OVERBERG, B. E. MORETTI, R. E. SLOVACEK, R. C. BLOCK, "Photoneutron Target Development for the RPI Linear Accelerator," *Nucl. Instrum. Meth. A*, **438**, 253 (1999).
6. Kamis Incorporated, Certification No. 005009-A, Mahopac Falls, New York.
7. R. C. BLOCK, P. J. MARANO, N. J. DRINDAK, F. FEINER, K. W. SEEMANN, and R. E. SLOVACEK, "A Multiplicity Detector for Accurate Low-Energy Neutron Capture Measurements," *Proc. Int. Conf. Nuclear Data for Science and Technology*, May 30-June 3, 1988, Mito, Japan, p. 383.
8. D. P. BARRY, "Neodymium Neutron Transmission and Capture Measurements and Development of a New Transmission Detector," PhD Thesis, Rensselaer Polytechnic Institute (2003).
9. G. LEINWEBER, D. P. BARRY, J. A. BURKE, M. J. RAPP, R. C. BLOCK, Y. DANON, J. A. GEUTHER, and F.J. SAGLIME III, "Europium resonance parameters from neutron capture and transmission measurements in the energy range 0.01–20 MeV," *Ann. Nucl. Energy*, **69**, pp. 74 - 89, (2014).
10. R. C. BLOCK, M. C. BISHOP, D. P. BARRY, G. LEINWEBER, R. V. BALLAD, J. A. BURKE, M. J. RAPP, Y. DANON, A. YOUMANS, N. J. DRINDAK, G. N. KIM, Y.-R. KANG, M. W. LEE and S. LANDSBERGER, "Neutron transmission and capture measurements and analysis of Dy from 0.01 to 550 eV," *Prog. Nucl. Energ.*, **94**, pp. 126-132, (2017).

11. B. E. EPPING, G. LEINWEBER, D. P. BARRY, M. J. RAPP, R. C. BLOCK, T. J. DONOVAN, Y. DANON, and S. LANDSBERGER, "Rhenium Resonance Parameters from Neutron Capture and Transmission Measurements in the Energy Range 0.01 eV – 1 keV," *Prog. Nucl. Energ.*, **99**, pp. 59-72, (2017).
12. Y. DANON, "Design and Construction of the RPI Enhanced Thermal Neutron Target and Thermal Cross Section Measurements of Rare Earth Isotopes," PhD Thesis, Rensselaer Polytechnic Institute (1993).
13. N. M. LARSON, "Updated Users' Guide for SAMMY: Multilevel R-Matrix Fits to Neutron Data Using Bayes' Equations," ORNL/TM-9179/R8 ENDF-364/R2, Oak Ridge National Laboratory (October 2008).
14. M. B. CHADWICK et al., "ENDF/B-VII.1: Nuclear Data for Science and Technology: Cross Sections, Covariances, Fission Product Yields and Decay Data," *Nucl. Data Sheets*, **112**, 2887 (2011).
15. A. SANTAMARINA, D. BERNARD, P. BLAISE, M. COSTE, A. COURCELLE, T. D. HUYNH, C. JOUANNE, P. LECONTE, O. LITAIZE, S. MENGELLE, G. NOGUERE, J.-M. RUGGIERI, O. SEROT, J. TOMMASI, C. VAGLIO, and J.-F. VIDAL, JEFF Report 22 (Nuclear Energy Agency Organisation for Economic Co-operation and Development, 2009).
16. K. SHIBATA, O. IWAMOTO, T. NAKAGAW, N. IWAMOTO, A. ICHIHARA, S. KUNIEDA, S. CHIBA, K. FURUTAKA, N. OTUKA, T. OHASAWA, T. MURATA, H. MATSUNOBU, A. ZUKERAN, S. KAMADA, and J.-I. KATAKURA, *J. Nucl. Sci. Technol.*, **48**, 1 (2011).
17. Y. DANON and R. C. BLOCK, "Minimizing the Statistical Error of Resonance Parameters and Cross Sections Derived from Transmission Measurements," *Nucl. Instrum. Meth. A*, **485**, 585 (2002).
18. S. F. MUGHABGHAB, *Atlas of Neutron Resonances*, 5th ed., Elsevier, New York (2006).